ELSEVIER

Journal of Power Sources 70 (1998) 59–69

JOURNAL OF POWER SOURCES

A review of impedance measurements for determination of the state-of-charge or state-of-health of secondary batteries

F. Huet

UPR 15 du CNRS, Physique des Liquides et Électrochimie, Université Pierre et Marie Curie, Tour 22, 4 Place Jussieu, 75252 Paris Cedex 05, France

Received 11 February 1997; accepted 19 May 1997

Abstract

A detailed review of the applicability of impedance measurement as a test of state-of-charge or state-of-health of battery cells has been performed in both scientific journals and technical conferences. The relationship between the various impedance parameters encountered in the literature has been investigated. Only studies concerning lead–acid and nickel–cadmium secondary battery cells, which are the most widely used batteries in industrial applications, have been considered. The rate capacities of the battery cells varied from 1 A h to several thousands of A h. © 1998 Elsevier Science S.A.

Keywords: Impedance; Conductance; Internal resistance; Lead–acid batteries; Nickel–cadmium batteries; State-of-charge; State-of-health; Residual capacity

1. Introduction

The impedance techniques have been widely used in the last two decades for investigating the kinetics of primary and secondary battery cells and determining their state-of-charge (SOC) or state-of-health (SOH). In scientific journals, most studies concern laboratory experiments carried out on small capacity cells. Since 1992, field experiments performed on high capacity cells have been reported in technical conferences (Intelec, Power Quality, American Power Conference, Power Sources Symposium...).

In the literature concerning batteries, the word impedance has different meanings. In the electrochemical field, it denotes the electrochemical impedance, defined as the transfer function between potential and current, which is a complex quantity and is usually measured using a frequency response analyzer. In electrical engineering, most often impedance denotes an electrical parameter, sometimes called internal resistance, whose signification depends on the measurement technique.

After describing the various impedance parameters, together with the measurement techniques, this paper shows what kind of information may be obtained from the impedance techniques and reviews the investigations undertaken for assessing the ability of these techniques for determining the SOC or SOH of secondary lead–acid and nickel–cadmium batteries.

PII S0378-7753(97)02665-7

2. Impedance parameters

In this section, the word 'battery' denotes either one battery cell or several cells in series.

2.1. Electrochemical impedance

The electrochemical impedance (or AC impedance) of a battery characterizes its dynamic behavior, that is, its response to an excitation of small amplitude [1,2]. In principle, any type of excitation signal may be used (sine wave, noise, step...). However, in practice, sine waves are most of time employed. In galvanostatic mode, the d.c. current I (polarization current) charging or discharging the battery is controlled and a sinusoidal current:

$$\Delta I = I_{max} \sin(2\pi ft) \quad (1)$$

at frequency f, is superimposed to I, yielding a sinusoidal voltage response:

$$\Delta V = V_{max} \sin(2\pi ft + \phi) \quad (2)$$

around the d.c. voltage V at the terminals of the battery. The amplitude V_{max} and the phase angle ϕ depend on the frequency f. On the contrary, in potentiostatic mode, the d.c. voltage V at the terminals of the battery is controlled and a sinusoidal voltage:

$$\Delta V = V_{max} \sin(2\pi ft) \quad (3)$$

at frequency f is superimposed to V, yielding a sinusoidal current response:

$$\Delta I = I_{max} \sin(2\pi ft - \phi) \quad (4)$$

around the d.c. current I flowing through the battery. In that case, the amplitude I_{max} and the phase angle ϕ depend on the frequency f. In both cases, the impedance is defined by:

$$Z(f) = \frac{V_{max}}{I_{max}} e^{j\phi} \quad (5)$$

Therefore, the electrochemical impedance of a battery is a frequency-dependent complex number characterized either by its real and imaginary parts, or by its modulus $|Z| = V_{max}/I_{max}$ and its phase angle ϕ.

It must be noticed that the voltage amplitude V_{max} must not exceed about 10 mV to ensure that impedance measurements are performed in linear conditions. In that case, the excitation and response signals are actually sine waves, and the measured impedance does not depend on the amplitude of the excitation signal. Such condition is easily fulfilled in potentiostatic mode where V_{max} is directly imposed by the experimenter. In galvanostatic mode, I_{max} must be determined so that V_{max} is close to 10 mV at all frequencies, especially at the lowest analyzed frequency where the impedance modulus of a battery is maximum. High power a.c. currents (several A) may be required for high capacity batteries whose impedances are in the mΩ range.

2.1.1. Measurement techniques

Till the end of the seventies, a.c. bridges and lock-in amplifiers were used for impedance measurement [3,4]. From 1977 [5], most investigations were performed with frequency response analyzers based on harmonic analysis. In some cases, white noise was used as an excitation signal in conjunction with Fourier transform signal analyzers. Robinson [6,7] also used the background noise due to time-varying changes in the load of batteries connected to operating equipment. If small-sized equipment is required, as for space applications, the impedance modulus may be obtained by measuring V_{max} and I_{max} with simple root mean square (RMS) voltmeters [8].

Great care must be taken for measuring the low impedances of high capacity batteries. The connecting lead and connector impedances are significant compared to the battery impedance [9]; the measurement procedure must be improved by using four leads, two for the current flow and the other two for the voltage. Another point concerns the selection of the current-measuring resistor inside the electrochemical interface (galvanostat or potentiostat); the inductive behavior of resistances lower than 0.1 Ω induces errors in the impedance measurement at high frequency [10].

In many investigations, batteries were charged or discharged until the required SOC was reached; then, the current was switched off and, after a period of rest, that is, once the equilibrium was reestablished, the impedance measurement was performed in potentiostatic mode at open circuit voltage. Several authors have disagreed with this measurement procedure, arguing that the processes at equilibrium are different from those involved during the charge or discharge. They suggested to carry out impedance measurement while the battery was charging or discharging, that is under nonzero current control [5,11,12]. In that case, errors may appear since the nonstationarity behavior of the battery induces voltage drift. These errors, which depend on the rate at which the system changes, increase with the measurement period, and, therefore, become significant for the lowest analyzed frequencies. Improvements may be obtained by high-pass filtering the current and voltage signals before data processing in the frequency response analyzer [13]. Four dimensional nonstationary impedance analysis, which is based on consecutive measurements of a series of impedance diagrams in a given frequency range, also enables correction of the errors caused by the system evolution [12,14,15].

2.1.2. Impedance diagrams

Impedance diagrams may be plot in the Bode plane (modulus in log scale vs. frequency and phase angle vs. frequency) or, more frequently, in the Nyquist plane (imaginary part vs. real part). In the latter case, electrochemists are used to plot the opposite of the imaginary part on the ordinate axis, so that the capacitive loops appear in the upper quadrants.

The general shape of the Nyquist diagram of the complex electrochemical impedance of a large capacity lead–acid battery cell is given in Fig. 1. This diagram presents:

- an inductive part at frequencies higher than 100 Hz;
- a high frequency resistance R_{HF} in the range of mΩ,

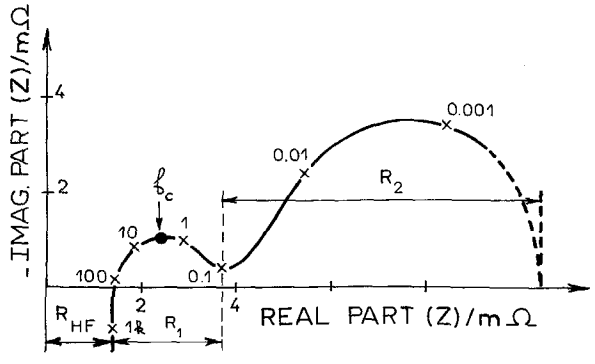

Fig. 1. Shape of the Nyquist diagram of the complex impedance of a large capacity lead–acid battery cell (frequencies in Hz).

which is the real part of the impedance at frequencies higher than 100 Hz;
- a first and small capacitive loop (size R_1) for frequencies between 0.1 and 100 Hz;
- a second and large loop (size R_2) for frequencies lower than 0.1 Hz.

2.2. Conductance and internal resistance of batteries

In the literature, other electrical parameters, more or less related to the electrochemical impedance are also employed. The terminology is rather fluctuating, and, sometimes, it is hard to understand which quantity is actually measured.

The conductance is defined as the real part of the reciprocal of the impedance. If the phase angle ϕ is low, the conductance, which is given in Ω^{-1} or mho or siemens, is the reciprocal of the high-frequency resistance R_{HF}.

Several definitions of the internal resistance have been reported, each depending on the measurement technique. This resistance is usually measured either with a milliohmmeter or with the period-of-rest technique or with the current-pulse technique [16,17]. In the former case, a high frequency (typically 1 kHz) sinusoidal signal is employed and the milliohmmeter gives the real part of the complex electrochemical impedance, that is R_{HF} with the notations of Fig. 1. In the period-of-rest technique, the charging or discharging current I is switched off, yielding, after a period of rest T, a change ΔV in the potential of the battery cell. The internal resistance is then defined as the ratio $\Delta V/I$. In the current-pulse technique, a current pulse ΔI is applied during the battery charge or discharge under constant current, inducing, after time T, a voltage change ΔV. This leads to another definition of the internal resistance as the ratio $\Delta V/\Delta I$. In the last two cases, the internal resistance strongly depends on the time T.

(i) if ΔV is instantaneously measured ($T < 10$ ms), only the ohmic effects are involved; therefore, $\Delta V/I$ and $\Delta V/\Delta I$ are equal to the high frequency resistance R_{HF}.
(ii) if T is about 1 s, processes with time constants up to 1 s are also involved, such as penetration of the current lines in the pores of the electrodes. Therefore, $\Delta V/I$ and $\Delta V/\Delta I$ depend on the parameters R_{HF} and R_1 of Fig. 1. The contribution of R_1 is strongly related to T and cannot be quantified with the only measurement of $\Delta V/I$ or $\Delta V/\Delta I$.
(iii) if T is much longer, for example a few minutes, $\Delta V/I$ and $\Delta V/\Delta I$ also include the effects with longer time constants, such as mass transport in the electrolyte. Then, $\Delta V/I$ and $\Delta V/\Delta I$ depend on all parameters R_{HF}, R_1 and R_2 in a complicated way.

In cases (ii) and (iii), the impedance parameter is neither a pure resistance, nor the modulus of the electrochemical impedance at a given frequency. As already stated, it strongly depends on the time T, i.e., on the measurement procedure.

The period-of-rest and current-pulse techniques, which can be carried out at a much lower price than the electrochemical impedance technique, are usually employed for investigating a possible relationship between the impedance parameters $\Delta V/I$, $\Delta V/\Delta I$ and the SOC or SOH of batteries, without trying to relate the changes in these parameters with the electrochemical processes involved in the batteries. If information on the kinetics of these processes are required, the electrochemical impedance technique should be preferred.

3. Interest of battery impedance measurement

The investigation of the evolution of the impedance diagram of a battery cell with SOC or SOH allows in principle, first, the interpretation and quantification of the impedance diagram changes in relation with the changes in electrode porosity, electrode sulphatation, electrolyte concentration, and, second, the determination of a parameter (such as $|Z|$ or ϕ at a given frequency or R_{HF}, R_1, R_2 in Fig. 1), if it exists, which could be related to SOC or SOH.

3.1. Investigation of battery kinetics

Numerous investigations on the kinetics of the electrochemical processes involved in battery cells have been reported, for lead–acid cells [5,12,18–25] as well as for nickel–cadmium cells [11,26]. After some discussions about the interpretation of the impedance diagrams, the following ideas are generally admitted to explain the Nyquist diagram of a battery cell (Fig. 1): (a) the inductive part at frequencies higher than 100 Hz is attributed to the electrode geometry and to the connections inside the cell; (b) the ohmic resistance R_{HF} is due to the connections, the separator, the electrolyte resistivity and the surface coverage of the electrodes by crystallized lead sulphate; (c) the small capacitive loop (size R_1) is related to the porosity of the electrodes; (d) the large loop (size R_2) at low frequencies depends on the sulphatation reaction on the electrodes whose rate is controlled by mass transport of Pb^{2+} ions.

The equivalent circuit of a battery cell which is represented in Fig. 2 is widely accepted [3,27–29]. Subscripts p and n denote positive and negative electrodes, respectively. L_p and L_n are inductances, $R_{t,p}$ and $R_{t,n}$ represent the resistances of charge transfer at the electrodes, $C_{dl,p}$ and $C_{dl,n}$ are the capacitances due to space charge distribution in the electrochemical double layers, $Z_{w,p}$ and $Z_{w,n}$ are

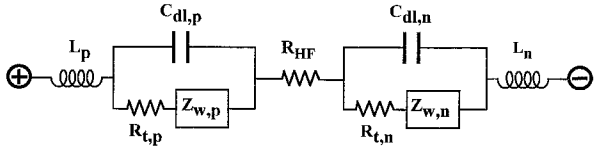

Fig. 2. Equivalent circuit of a battery cell.

Warburg impedances due to ion diffusion in the electrolyte and in the pores of the electrodes, and R_{HF} is the ohmic resistance mentioned above.

The impedance of a battery cell appears to be the sum of the ohmic resistance R_{HF} and of the impedances of the positive and negative electrodes:

$$Z_{cell} = Z_p + Z_n + R_{HF} \quad (6)$$

The determination of the kinetic parameters R_t, C_{dl} and mass transport parameters (thickness of the diffusion layer, diffusion coefficient) for each electrode cannot be achieved with the only measurement of the impedance of the battery cell. Even if nonlinear least squares fitting programs fit the data fairly well at a given potential, the parameters obtained do not follow regular trends with voltage and cycle history since the individual electrodes do not vary with potential in the same way [30]. The impedances of the positive and negative electrodes have to be measured separately. This is possible by using a reference electrode. The impedance of the positive (respectively negative) electrode is obtained if the voltage signal is measured between the positive (respectively negative) electrode and the reference electrode. As shown in Fig. 3a, the two electrodes of a fully charged lead–acid battery have impedances with different magnitude. It is clear that the impedance diagram of the cell does not enable separation of the contribution of each electrode in a single way.

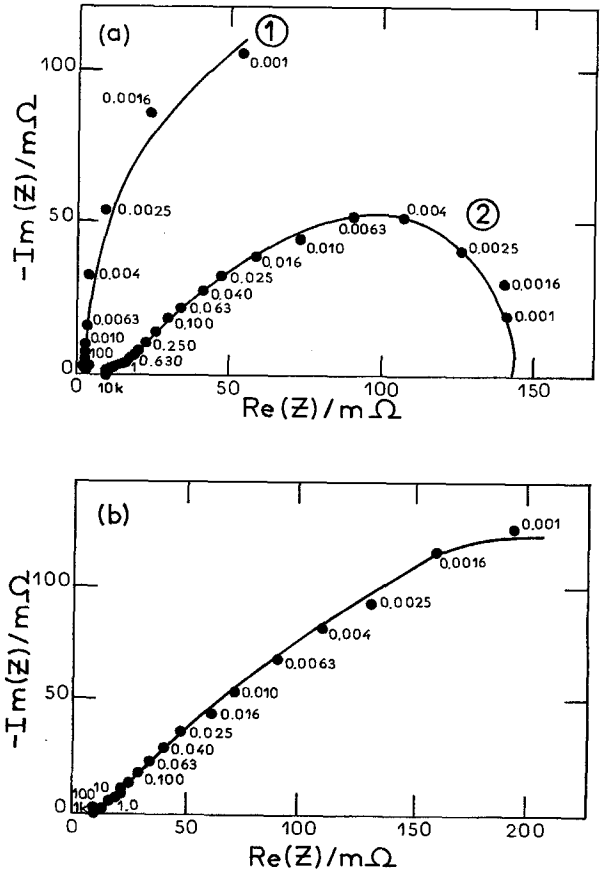

Fig. 3. The impedance diagrams of a fully charged lead–acid battery (6 V, 7 A h). Polarization current $I = 0$. (a) Curve 1 : positive plate; curve 2: negative plate. (b) The sum of a-1 and a-2 curves giving one-third of the measured impedance of the battery (from Ref. [5]).

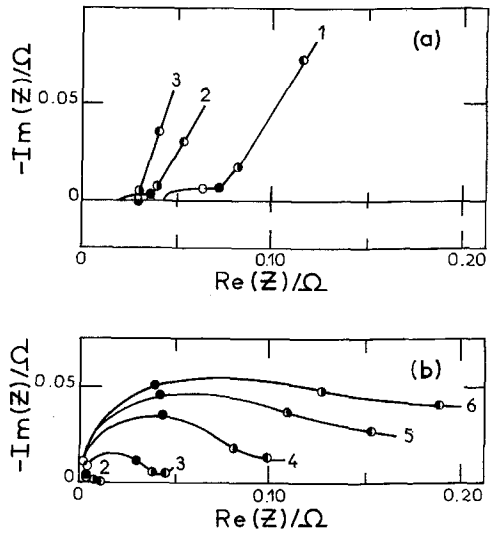

Fig. 4. Impedance characteristics of (a) positive and (b) negative electrodes of a model sealed lead–acid cell at different applied charges, C_c / C_d, equal to 1, zero; 2, 0.6; 3, 0.9; 4, 1.15; 5, 1.45; 6, 1.95. The following symbols denote frequencies: ○, 10 Hz; ●, 1 Hz; ◑, 0.1 Hz; ◐, 0.01 Hz. Symbols C_c and C_d denote charge and discharge, respectively (from Ref. [23]).

The contribution of the individual electrodes to the cell impedance depends, obviously, on the electrochemical system investigated, and also on the SOC of the cell. Jindra et al. [23] have measured the impedance of a model sealed 1.2 A h lead–acid cell and its electrodes in various experimental conditions. They have shown (see Fig. 4) that during the first half of galvanostatic charging, the cell impedance is controlled mainly by the positive electrode while at higher SOC and during overcharging the negative electrode was much more impedant. However, the ohmic resistance R_{HF} of the cell is given essentially by the resistance of the positive electrode in the whole range of SOC.

Other examples on the use of reference electrodes for kinetics investigation are reported for lead–acid batteries [5,12,22] and for nickel–cadmium batteries [28]. Reid [28] proposed to use the cell case as a reference electrode on flightweight Ni/Cd cells to separate the cell impedance into the contributions of each electrode, allowing improved diagnosis of cell problems.

3.2. Determination of parameters related to SOC or SOH

Parameters likely to be related to the SOC or SOH of a battery cell may be first derived directly from its impedance value at a given frequency, such as the impedance modulus $|Z|$, the phase angle ϕ, the real part $\mathrm{Re}(Z)$, the imaginary part $\mathrm{Im}(Z)$, the ohmic resistance which is $\mathrm{Re}(Z)$ at fre-

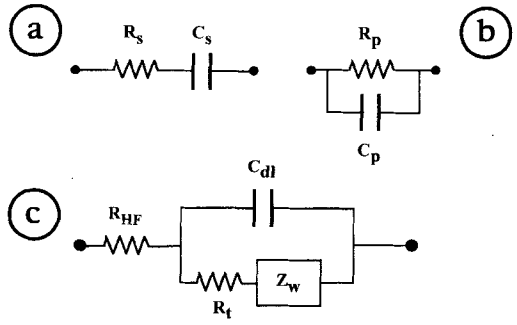

Fig. 5. Equivalent circuits of a battery cell.

quencies above 100 Hz. They also may be derived from the analysis of analog equivalent circuits of the battery cell.

The simplest circuit traducing the complex nature of the cell impedance is represented by a resistance and a capacitance in either a series mode (R_s = equivalent series resistance, C_s = equivalent series capacitance in Fig. 5a) or a parallel mode (R_p = equivalent parallel resistance, C_p = equivalent parallel capacitance in Fig. 5b) [3]. These electrical parameters are frequency-dependent.

$$Z(f) = R_s + \frac{1}{j2\pi f C_s} = \frac{R_p}{1 + j2\pi f R_p C_p} \quad (7)$$

Their dependence on SOC has been widely investigated in the early eighties [3,4] and more recently [31–33] since they require impedance at only one frequency, and, therefore, could lead to simple SOC testers. However, these parameters are no more used in the electrochemical studies concerning batteries because the fact that each frequency gives a resistance and a capacitance hinders any understanding of the electrochemical processes taking place in the cell. It must be emphasized that these resistance and capacitance have no electrochemical signification.

Other equivalent circuits used for determining a possible SOC-related impedance parameter are based on simplifications of the equivalent circuit of the battery cell shown in Fig. 2. The circuit represented in Fig. 5c is often employed [3,4,29,31,32,34] because its impedance diagram corresponds to that of Fig. 1. In this simplified circuit, the parameters R_t, C_{dl} and those related to mass transport are independent of frequency. Hence, a SOC tester based on the determination of any of these parameters would require advanced technologies since the impedance should be measured at several frequencies. It must be noticed that, except if one of the electrodes is much more impedant than the other (such as in nickel–hydrogen batteries), R_t and C_{dl} are not a charge transfer resistance and a double layer capacity, respectively, even if this terminology is sometimes used, since both positive and negative electrodes contribute to the cell impedance, as shown above.

4. Impedance as a SOC test: laboratory experiments

Research in laboratories of impedance parameters related to SOC or SOH of battery cells has been carried out for almost 20 years. Various parameters have been investigated for lead–acid and nickel–cadmium secondary batteries. The more typical and convincing results are presented.

4.1. Lead–acid batteries

Among the various parameters investigated, the ohmic resistance R_{HF} is perhaps the more attractive since its measurement may be performed in short times with simple instrumentation.

In 1981, Yahchouchi [35] and Gabrielli et al. [36] showed that the impedance of a large capacity lead–acid battery cell (2 V, 390 A h) increased when discharged. Fig. 6 shows that both parameters R_{HF} and R_1 defined in Fig. 1 increased with decreasing SOC. The increase of R_{HF} was attributed to decreasing electrolyte conductivity and increasing surface coverage of the electrodes by insulating crystallized lead sulphate. The increase of R_1, which depends on the porosity of the electrodes, was likely caused by a blocking of the pores by lead sulphate crystals and by bubbles when overcharging. Yahchouchi [35] thought that R_{HF} could inform on the battery SOC for continuous discharges not interrupted by short recharges which could dissolve the insulating crystals on the electrodes. He then proposed the use of R_1 as a SOC test and R_{HF} as a SOH test for stationary batteries operating in floating conditions. Indeed, since R_{HF} includes the resistance of internal connections, ohmic resistance increases might enable detection of internal damages due to corrosion. He concluded that it

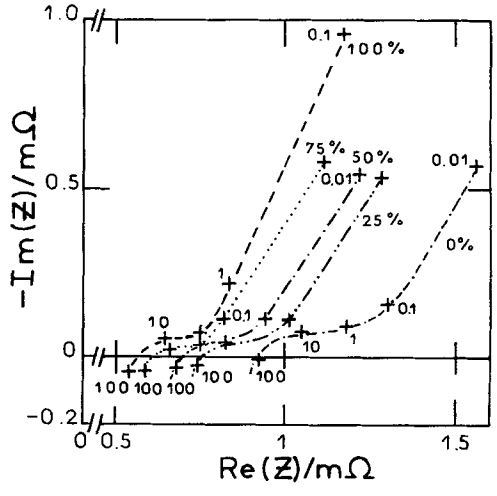

Fig. 6. Impedance diagrams of a 2 V, 390 A h tubular lead–acid battery cell at various SOC. Impedance measured at zero current after a rest of 3 days (from Ref. [36]).

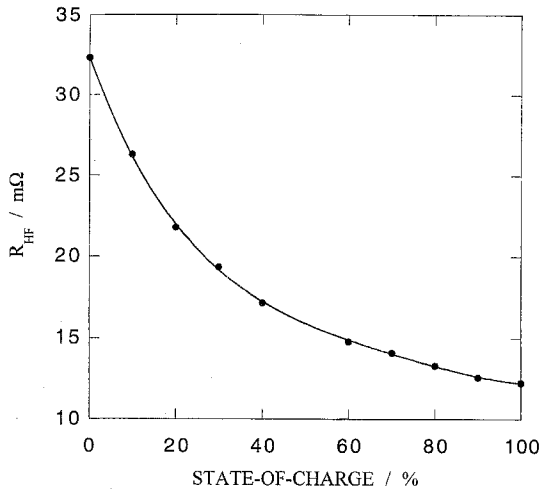

Fig. 7. Change in ohmic resistance of a 6 V, 2.6 A h lead–acid battery with SOC. Impedance measured at open circuit voltage after a rest of 1 h. (from Ref. [22]).

might be possible to define an upper limit of the ohmic resistance for each type of battery and control the battery health periodically by comparing the measured value of R_{HF} to this upper limit.

Barton and Mitchell [22] also found correlation of the ohmic resistance with the SOC of small capacity lead–acid batteries (Fig. 7). The ohmic resistance change was attributed essentially to the change in electrolyte specific gravity during charge or discharge. They observed that the ohmic resistance of a flooded cell with plates at various SOC and sulphuric acid concentration held constant, remained unchanged at all SOC. The same behavior was obtained with a sealed 6 V, 100 A h battery.

In 1986, Hughes et al. [29] proposed another method for estimating the SOC of fully sealed lead–acid battery cells. They observed no consistent change with SOC in the parameters defined in the analogue circuit shown in Fig. 5c, and no single frequency impedance determination liable to provide a basis for a test. However, the product of the 'charge transfer resistance' R_t and the 'double layer capacity' C_{dl} was found to correlate with the residual charge for new (about 2 years) and old (about 9 years) cells. By the way, it must be remembered that R_t and C_{dl} should not be termed 'charge transfer resistance' and 'double layer capacity' because the equivalent circuit of the impedance cell employed for data fitting includes both positive and negative electrodes whose evolutions with SOC may not be similar, as stated above. Fig. 8 shows an excellent estimation in the residual capacity range 50 to 100%. In Fig. 8a, R_t and C_{dl} were obtained by fitting the impedance diagram with the analogue circuit shown in Fig. 5c and were corrected for porosity. In Fig. 8b, the product was derived with the following relationship:

$$R_tC_{dl} = \frac{1}{2\pi f_c} \quad (8)$$

where f_c is the frequency at the top of the high frequency semi-circle in the Nyquist impedance diagram (see Fig. 1). A SOC test based on f_c determination would require simple instrumentation since the isolation of the time constant $1/2\pi f_c$ may be obtained in a few seconds using fast Fourier methods. The basic difference observed in Fig. 8 with differently aged and differently treated cells was attributed to different wears produced on the positive plates with the generation of more fine particles. The impedance parameter could then be a useful measure of cell aging.

In a further work on large 25 A h, spiral-wound, fully sealed lead–acid cells [34], the authors observed that the SOC test parameter R_tC_{dl} seemed to be independent of cycle number, discharge rate, and age of the cell and could also be used to indicate the SOH of such cells.

Recently, Jindra et al. [23] have measured the impedance of a model hermetic 1.2 A h lead–acid battery cell and its electrodes by using a reference electrode. They monitored the impedance at 0.1 Hz and, at the same time, the potential of the electrodes, the cell voltage, and the oxygen overpressure during continuous galvanostatic charging at a

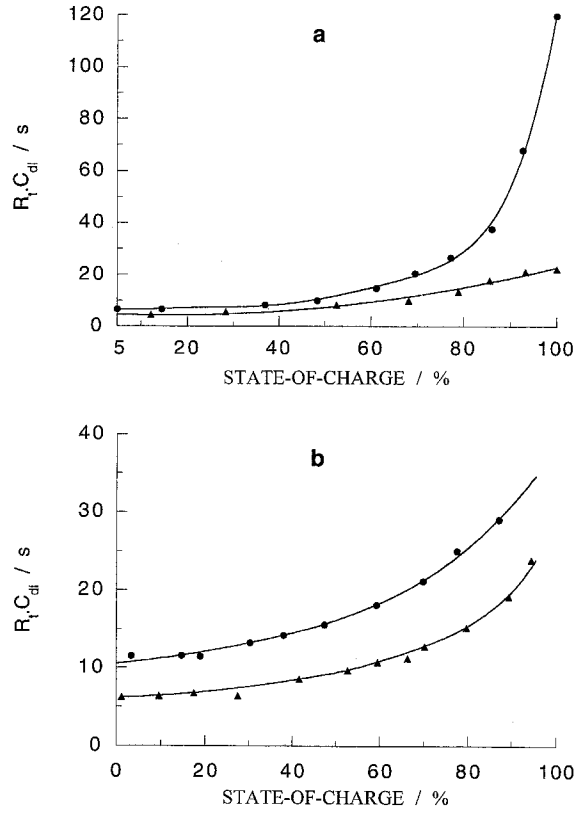

Fig. 8. Relationship of R_tC_{dl} to residual capacity for the (●) new and (▲) old cells. (a) from the data obtained using the analogue circuit shown in Fig. 5c; (b) directly from the experimental impedance from the reciprocal of the frequency at the top of the high frequency semi-circle (from Ref. [29]).

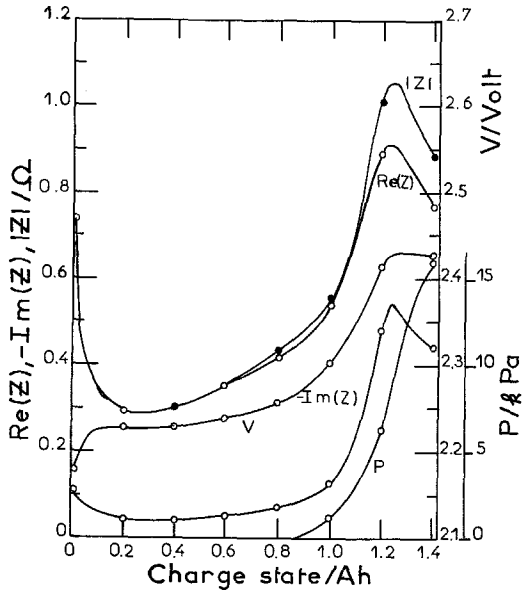

Fig. 9. Evolution of impedance characteristics (modulus |Z|, real part Re(Z), imaginary part Im(Z)) at 0.1 Hz, voltage V, and overpressure P of a model sealed 1.2 A h cell during galvanostatic charging at a C6 rate (from Ref. [23]).

C6 rate. Fig. 9 shows a characteristic decrease of the impedance modulus during the internal pressure increase, indicating that the state of full charge was reached. The peak impedance was sensitive to charging current and temperature but the character of the curve was preserved. Hence, a test of full charge based on impedance modulus monitoring, which requires a rather simple equipment, could be envisioned.

In conclusion, various impedance parameters were investigated in laboratory experiments and most authors are rather optimistic concerning the ability of the impedance technique to provide a SOC test. Nevertheless, some authors found that the impedance diagrams were too much sensitive to temperature variations [13]. These authors consider that the impedance is not a practical technique for field uses, and must be applied in controlled laboratory environment for studying the internal mechanisms of the batteries. However, a careful look at their results shows that the ohmic resistance was independent of temperature variations and could be the proper impedance parameter to use as a SOC test.

4.2. Nickel–cadmium batteries

Similar impedance parameters have been tested for the determination of the SOC of nickel–cadmium battery cells.

Concerning the ohmic resistance, slighter variations with SOC were expected. As the concentration of hydroxide ions remains constant during charge and discharge, the contribution of the electrolyte might be unimportant. Lahav and Appelbaum [8] measured the impedance modulus of 7 A h nickel–cadmium battery cells for low earth orbit applications, at high rates and low temperatures. The impedance measurements were carried out at high frequency and, since low impedance phase angles were obtained, the impedance parameter was essentially the ohmic resistance. An excellent correlation between this parameter, the SOC, and the operating temperature T was obtained (Fig. 10), so that the authors proposed an empirical equation:

$$R_{HF} = K_0 + K_1 T + (K_2 + K_3 T)\mathrm{SOC} \quad (9)$$

where K_i are fitting coefficients, which could serve as an indicator of the battery SOC during missions in space. It must be emphasized that the R_{HF} variations with SOC were fairly small (about 10%) compared to those obtained with lead–acid batteries. This probably explains the conflicting conclusions concerning the ability of the ohmic resistance to follow the SOC of nickel–cadmium batteries.

For small 0.85 A h cylindrical sealed nickel–cadmium battery cells at room temperature, Blanchard [11] also observed small variations of ohmic resistance with SOC (about 20%) during discharge at C1 rate. Furthermore, no significant R_{HF} variation was measured during charge at the same rate, except when overcharging where oxygen bubbles in the electrolyte slightly increased the ohmic resistance. The difference between the values of R_{HF} at the beginning of the discharge and at the end of the charge could be explained either by removal of the oxygen bubbles during the period of rest at open circuit voltage, or by relaxation processes, e.g., diffusion, which allows a uniform concentration of electrolyte to be reestablished throughout the cell. Wider variations were observed for the charge transfer resistance R_t, the double layer capacity C_{dl}, and the impedance modulus at given frequencies. As for lead–acid batteries [23], the monitoring of the impedance modulus at 1 Hz during charge at C1 rate allowed determination of the full charge state (Fig. 11a). On the other hand, the rapid increase of the impedance modulus during discharge at C1 rate indicated that approximately 15% of the initial capacity was still available (Fig. 11b).

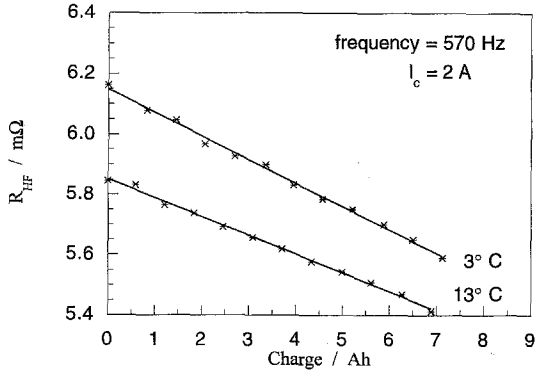

Fig. 10. Internal impedance modulus of a 7 A h nickel–cadmium battery cell as a function of SOC at charge current I_c of 2 A and frequency of 570 Hz (from Ref. [8]).

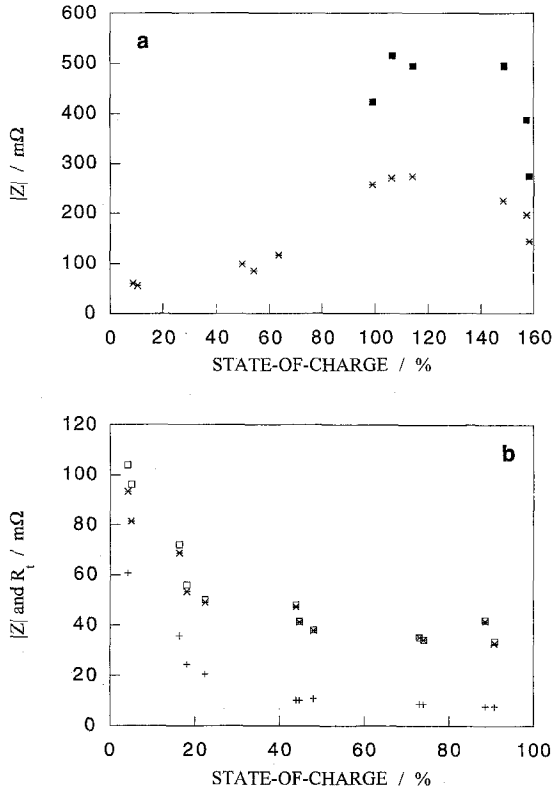

Fig. 11. Evolution of the impedance modulus as a function of SOC during (a) charge at C1 rate: (∗) |Z| at 1 Hz, (■) |Z| at 0.4 Hz, and (b) discharge at C1 rate: (∗) |Z| at 1 Hz, (□) |Z| at 0.4 Hz, (+) R_t (from Ref. [11]).

Other impedance parameters were investigated with rather conflicting results, such as the imaginary part of the impedance at given frequencies [9,31].

5. Impedance as a SOH test: field experiments

In industrial applications, the estimation of the residual capacity of secondary batteries is convoluted since the batteries are subject to aging because of loss of active material, corrosion, poor maintenance, etc. The question may be the evaluation of the SOH of the battery, that is, its actual capacity after recharge, or its SOC, that is, the effective capacity which could be provided during immediate discharge. In many applications, such as in the uninterruptible power supply systems, where reserve batteries are used in case of commercial a.c. power loss, only the SOH of these batteries is under question, since they operate in floating conditions and are continuously recharged.

Very few thorough investigations of impedance parameter related to battery SOH in research laboratories have been reported [37–40]. From 1992, large-scale field experiments have been undertaken under the impulse of impedance/conductance tester manufacturers, Midtronics and AVO-Biddle Instruments. First, valve regulated lead–acid (VRLA) batteries were studied [41–43]. These 'maintenance-free' batteries, which had demonstrated a rapid expansion in many areas of battery usage, urgently required a technique for capacity evaluation. Traditional techniques used for flooded vented cells, such as specific gravity measurement, visual inspection of grid corrosion and internal problems, electrolyte level checking, could not be applied because these cells are sealed. The only reliable procedure to detect premature capacity failures was the discharge test at constant current to a specified terminal voltage, which is expensive, time consuming and leaves the batteries to be tested out of service for an extended period of time.

In the last 3 years, many results have been published concerning both gelled electrolyte (GEL) and absorbed glass mat (AGM) VRLA batteries [44–52], flooded lead–acid batteries [44,46,48,53,54] and nickel–cadmium batteries [44] in various applications (telecommunications, UPS equipment, electric power utility, automobile, railroad signalling, etc.).

Commercially available impedance/conductance testers use a single-frequency excitation signal. Differences exist in the waveform (alternating current at a fixed frequency or square-shaped current pulse) and in the frequency of the excitation signal (1000 Hz for the Hewlett-Packard 4328A, 60 Hz for the BITE of Biddle Instruments, about 10 Hz for the Celltron and about 25 Hz for the Midtron of Midtronics). Variations may be also noted in the algorithms used for data processing (the HP 4328A gives the impedance real part, the BITE gives the impedance modulus, and the Midtronics products give the real part of the impedance reciprocal). All these testers use the four-wire technique and some of them are able to make on-line measurements. Other hand-held electronic devices based on impedance/internal resistance measurement have been developed for battery capacity estimation [48,52,55].

AC-impedance diagrams of large flooded lead–acid batteries with characteristic frequency f_c at the top of the high-frequency semi-circle (see Fig. 1) varying from approximately 200 Hz to 1.5 Hz have been reported by Robinson [56]. As a consequence, the impedance parameter measured by an impedance/conductance tester not only depends on the value of the fixed frequency of the test signal and the algorithm used in data processing, but also depends on the characteristics of the battery cell (type, rated capacity, electrode configuration). In other words, different testers measure different impedance parameters for the same cell whereas a given tester does not measure the same impedance parameter on all types of battery cells.

However, since all commercial testers perform measurements at relatively high frequencies (above 10 Hz), the impedance parameter is, roughly speaking, close to the ohmic resistance R_{HF} of the battery cell. Nevertheless, extensive comparisons between the results given by the impedance/conductance testers exhibit systematic deviations between the conductance values and the reciprocal of

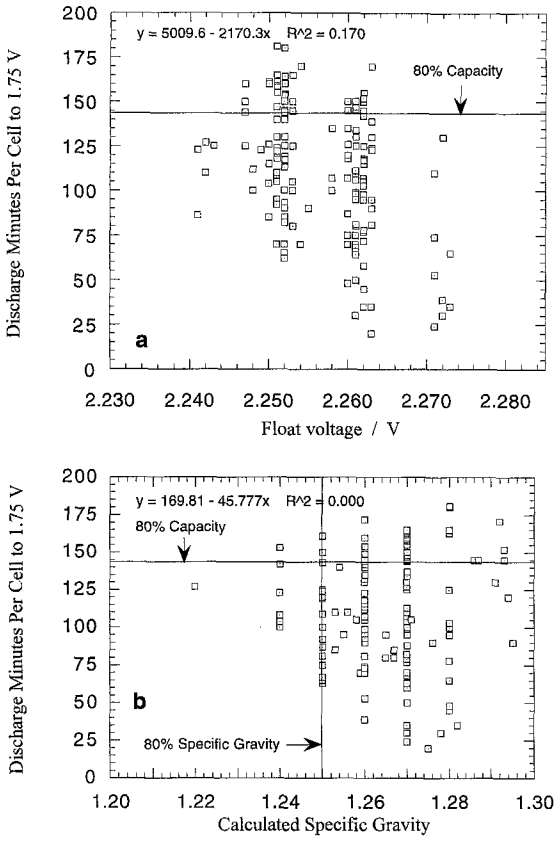

Fig. 12. Discharge capacity vs. (a) float voltage and (b) calculated specific gravity for seven strings (168 cells of 1000 A h); string nos. 9–15; 263 A to 1.75 V per cell (from Ref. [46]).

the impedance values [45,49]. Heron et al. [49] also found a partial repeatability in results for each tester, which indicates the strong difficulties to precisely measure such low impedance values.

In cooperation with Midtronics, Feder and Hlavac [50,57], Feder et al. [41,42,46,51], Hlavac and Feder [58,59] and Hlavac et al. [44,54] have published numerous papers in the 1992–1996 period based on the most significant study of VRLA battery capacity and conductance ever undertaken in field and laboratory experiments. Their results have shown remarkable correlation of the conductance of a battery and its capacity performance measured by a discharge test. They have also demonstrated the ability of the conductance to identify potential premature capacity failure. Typical results on VRLA batteries of a large (15 strings, 24 cells each, 1000 A h cell) telecommunications transmission plant are presented [41,46]. Fig. 12 shows that the discharge time in the capacity test (263 A rate to 1.75 V per cell) was correlated neither with individual cell float voltage, nor with specific gravity determined indirectly by measurement of cell open-circuit voltage with the relationship:

calculated specific gravity

$$= \text{cell open} - \text{circuit voltage} - 0.85 \qquad (10)$$

It is noteworthy that all values of float voltage were within the narrow manufacturer's allowed range of variation, while a much wider capacity distribution was observed (from 20 to 180 min) with many cells under the 80% capacity limit (rated capacity = 180 min to 1.75 V at 263 A discharge rate). On the contrary, a fairly good correlation was observed between the discharge capacity and the conductance measured prior the discharge test (Fig. 13a), with a correlation coefficient $R^2 = 0.825$. The results were summarized in the 'box-score' (Fig. 13b), which may be used as a predictive tool. The horizontal line (80% capacity) in Fig. 13a intersects the regression line at 2.55 kmho conductance, where a vertical line is drawn, marking the conductance cut-off value. The box-score, which contains the number of cells in each quadrant of Fig. 13a, indicates that conductance provides an overall (bad + good) successful prediction rate of 88% and has a 98% success rate in predicting capacity failures. Deriving the cut-off conductance value from a single string discharge and comparing this value to the measured conductance of cells of the same size and design in other strings, Feder and Hlavac [57] and Hlavac et al. [44] obtained accuracies around 90% in detecting cells with capacity less than 80%. Other procedures have been evaluated to select the most effective technique for detecting cell failures, including the proper choice of the conductance cut-off value [50] and the possibility of single or multiple cell on-line conductance measurements [59].

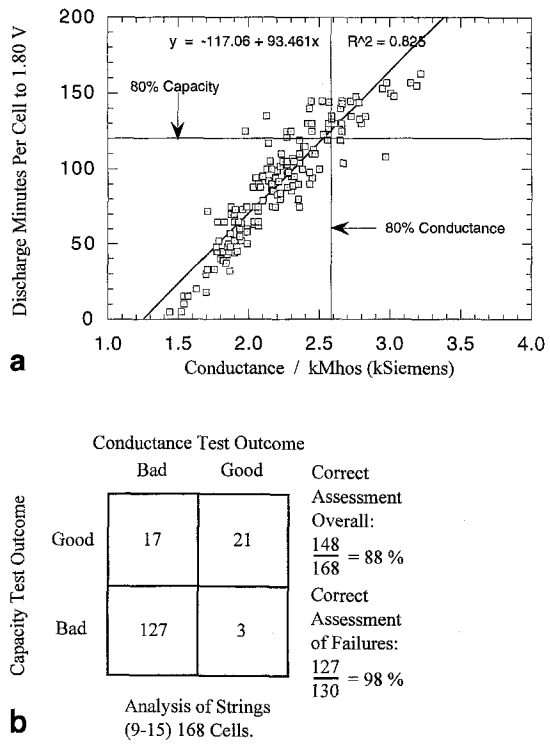

Fig. 13. (a) Discharge capacity vs. conductance and (b) box score of conductance vs. capacity outcome for seven strings (168 cells of 1000 A h); string nos. 9–15; 263 A to 1.8 V per cell (from Ref. [46]).

Such convincing results have not been obtained by all investigators performing large-scale field experiments. Misra et al. [45,60] found no close correlation between impedance/conductance and capacity of VRLA batteries. They consider that impedance/conductance measurements cannot predict battery capacity and may only determine gross defects such as dropped plates, severe grid corrosion or extreme dry-out. Heron et al. [49] also claimed that impedance/conductance testing is not a perfectly accurate measure of the battery health, because of the number of variables and potential sources of error in the impedance testing. They thoroughly studied the sources of error affecting the relationship between impedance/conductance and capacity, or the reproducibility of impedance/conductance measurements. Furthermore, effects of ambient temperature and SOC of the battery on the impedance/conductance measurements have been reported [47,49,61]. The variations induced by temperature have been evaluated to less than 10% in absolute terms over the range (25°C, 75°C) [61]. To prevent SOC influence, the batteries should be fully recharged prior to impedance/conductance measurements [49].

In conclusion, all authors agree that impedance/conductance testing is a useful tool in detecting potential problem cells which require further investigation. Most of the authors consider that discharge testing remains the only accurate method of assessing the SOH of Batteries.

6. Conclusions

A review of the investigations undertaken for assessing the ability of impedance testing for determining the SOC or SOH of lead–acid and nickel–cadmium batteries in laboratory and field experiments has been performed in both scientific journals and conference papers. The drawing conclusions are the following: (1) The SOC and SOH undoubtedly influence the battery impedance; (2) Ambient temperature also affects the battery impedance, especially at low frequencies where the kinetics of the electrochemical processes is under diffusion control; (3) As a consequence, a SOC or SOH tester allowing field experiments in uncontrolled temperature environment should be based on high frequency impedance measurement (between 10 and 100 Hz) for determination of the ohmic resistance, or its reciprocal which is the conductance. In this frequency range, the influence of temperature is less than 10% of the absolute impedance/conductance value; (4) Lead–acid batteries exhibit ohmic resistance variations with residual capacity of about 100%, while much lower variations (of about 10%) were observed in nickel–cadmium batteries. This seems to preclude any use of impedance technique for SOH determination of nickel–cadmium batteries. Only gross defects could be detected; (5) The low values of ohmic resistance of large-capacity lead–acid batteries and their rather small range of variations (about 100%) yield some difficulties in reproducing accurate measurement; (6) Improvements in the calibration of commercially available impedance testers and standardization of the measurement procedure are still necessary to definitely verify whether impedance testing is able to assess the battery condition; (7) Nevertheless, the impedance technique allows detection of probable bad cells requiring further investigation; (8) No field experiment for determining SOC of lead–acid batteries with impedance technique has been performed. This question is convoluted since the SOH also influences the battery impedance.

Acknowledgements

The author would like to acknowledge the support of the European Community (Joule II, Contract No CT94-0410) and Dr. M. Keddam (UPR15, CNRS) for helpful discussions. He would like also to pay his respects to the memory of Dr. M. Imamura (WIP, München) who initiated this work.

References

[1] C. Gabrielli, Identification of electrochemical processes by frequency response analysis, Solartron, Technical Report No 4183, 120 p. (1983).
[2] N.A. Hampson, S.A.G.R. Karunathilaka, R. Leek, J. Appl. Electrochem. 10 (1980) 3–11.
[3] M.L. Gopikanth, S. Sathyanarayana, J. Appl. Electrochem. 9 (1979) 369–379.
[4] S. Sathyanarayana, S. Venugopalan, M.L. Gopikanth, J. Appl. Electrochem. 9 (1979) 125–139.
[5] M. Keddam, Z. Stoynov, H. Takenouti, J. Appl. Electrochem. 7 (1977) 539–544.
[6] R.S. Robinson, J. Power Sources 42 (1993) 381–388.
[7] R.S. Robinson, Proc. INTELEC Conf., Paris, France, 1993, pp. 365–368.
[8] D. Lahav, J. Appelbaum, J. Power Sources 38 (1992) 295–301.
[9] M. Hughes, R.T. Barton, S.A.G.R. Karunathilaka, N.A. Hampson, R. Leek, J. Appl. Electrochem. 15 (1985) 129–137.
[10] S.A.G.R. Karunathilaka, R.T. Barton, M. Hughes, N.A. Hampson, J. Appl. Electrochem. 15 (1985) 251–257.
[11] P. Blanchard, J. Appl. Electrochem. 22 (1992) 1121–1128.
[12] Z. Stoynov, B. Savova-Stoynov, T. Kossev, J. Power Sources 30 (1990) 275–285.
[13] P.R. Roberge, E. Halliop, G. Verville, J. Smit, J. Power Sources 32 (1990) 261–270.
[14] Z.B. Stoynov, B.S. Savova-Stoynov, J. Electroanal. Chem. 183 (1985) 133–144.
[15] Z. Stoynov, B. Savova-Stoynov, T. Kossev, J. Power Sources 30 (1990) 301–307.
[16] J.B. Copetti, F. Chenlo, Photovoltaic Solar Energy Conf., Montreux, Switzerland, 1992, pp. 1116–1119.
[17] J.B. Copetti, F. Chenlo, J. Power Sources 47 (1994) 109–118.
[18] C. Rakotomavo, PhD Thesis, Université Paris 7, France (1983).
[19] P. Casson, N.A. Hampson, M.J. Willars, J. Electroanal. Chem. 97 (1979) 21–32.
[20] S. Kelly, N.A. Hampson, K. Peters, J. Appl. Electrochem. 11 (1981) 765–769.

[21] N.A. Hampson, S. Kelly, K. Peters, J. Appl. Electrochem. 11 (1981) 751–763.
[22] R.T. Barton, P.J. Mitchell, J. Power Sources 27 (1989) 287–295.
[23] J. Jindra, M. Musilova, J. Mrha, A.A. Taganova, J. Power Sources 37 (1992) 403–409.
[24] M. Keddam, C. Rakotomavo, H. Takenouti, Proc. Symp. Advances in Lead–Acid Batteries, The Electrochemical Society, 14 (1984) 277–287.
[25] M. Keddam, C. Rakotomavo, H. Takenouti, J. Appl. Electrochem. 14 (1984) 437–448.
[26] R.T. Barton, M. Hughes, S.A.G.R. Karunathilaka, N.A. Hampson, J. Appl. Electrochem. 15 (1985) 399–404.
[27] X.Y. Xiong, H. Vander Poorten, M. Crappe, Electrochim. Acta 41 (1996) 1267–1275.
[28] M.A. Reid, J. Power Sources 29 (1990) 467–476.
[29] M. Hughes, R.T. Barton, S.A.G.R. Karunathilaka, N.A. Hampson, J. Appl. Electrochem. 16 (1986) 555–564.
[30] M.A. Reid, Electrochim. Acta 38 (1993) 2037–2041.
[31] V.V. Viswanathan, A.J. Salkind, J.J. Kelley, J.B. Ockerman, J. Appl. Electrochem. 25 (1995) 716–728.
[32] V.V. Viswanathan, A.J. Salkind, J.J. Kelley, J.B. Ockerman, J. Appl. Electrochem. 25 (1995) 729–739.
[33] M.S. Suresh, S. Sathyanarayana, J. Power Sources 37 (1992) 335–345.
[34] M. Hughes, R.T. Barton, S.A.G.R. Karunathilaka, N.A. Hampson, R. Leek, J. Power Sources 17 (1986) 305–329.
[35] N. Yahchouchi, PhD Thesis, Université Paris 6, France (1981).
[36] C. Gabrielli, M. Keddam, H. Takenouti, N. Yahchouchi, Proc. 160th Electrochemical Society Meeting, Denver, CO, 1981, Ext. Abst. Vol. 81-82, p. 20.
[37] S. DeBardelaben, Proc. INTELEC Conf., Toronto, Canada, 1986, pp. 365–368.
[38] F.J. Vaccaro, P. Casson, Proc. INTELEC Conf., Stockholm, Sweden, 1987, pp. 128–131.
[39] J. Alzieu, J. Leroy, A. Vicaud, Rev. Gén. Électrique 3 (1990) 50–55.
[40] J.M. Hawkins, R.G. Hand, Proc. INTELEC Conf., Boston, MA, 1996, pp. 640–645.
[41] D.O. Feder, T.G. Croda, K.S. Champlin, S.J. McShane, M.J. Hlavac, J. Power Sources 40 (1992) 235–250.
[42] D.O. Feder, T.G. Croda, K.S. Champlin, M.J. Hlavac, Proc. INTELEC Conf., Washington, DC, 1992, pp. 218–233.
[43] G.J. Markle, Proc. INTELEC Conf., Washington, DC, 1992, pp. 212–217.
[44] M.J. Hlavac, D.O. Feder, T.G. Croda, K.S. Champlin, Proc. INTELEC Conf., Paris, France, 1993, pp. 375–383.
[45] S.S. Misra, T.M. Noveske, L.S. Holden, S.L. Mraz, Proc. INTELEC Conf., Paris, France, 1993, pp. 384–391.
[46] D.O. Feder, M.J. Hlavac, W. Koster, J. Power Sources 46 (1993) 391–415.
[47] G.J. Markle, Proc. INTELEC Conf., Paris, France, 1993, pp. 444–448.
[48] J.M. Hawkins, Proc. INTELEC Conf., Vancouver, Canada, 1994, pp. 263–269.
[49] R. Heron, A. McFadden, J. Dunn, Proc. INTELEC Conf., Vancouver, Canada, 1994, pp. 270–281.
[50] D.O. Feder, M.J. Hlavac, Proc. INTELEC Conf., Vancouver, Canada, 1994, pp. 282–291.
[51] D.O. Feder, M.J. Hlavac, S.J. McShane, J. Power Sources 48 (1994) 135–161.
[52] Y. Konya, T. Takeda, K. Takano, M. Kohno, K. Yotsumoto, T. Ogata, Proc. INTELEC Conf., Vancouver, Canada, 1994, pp. 256–262.
[53] C.M. Gabriel, K.W. Uhlir, Proc. American Power Conf., Chicago, IL, 1993, Vol. 1, pp. 38–43.
[54] M.J. Hlavac, D.O. Feder, D. Ogden, Proc. American Power Conf., Chicago, IL, 1993, Vol. 1, pp. 44–57.
[55] M. Yamanaka, K. Ikuta, T. Matsui, H. Nakashima, Y. Tomokuni, Proc. INTELEC Conf., Kyoto, Japan, 1991, pp. 202–208.
[56] R.S. Robinson, Proc. INTELEC Conf., Boston, MA, 1996, pp. 654–661.
[57] D.O. Feder, M.J. Hlavac, Batteries Int. 18 (1994) 60–61.
[58] M.J. Hlavac, D. Feder, Proc. INTELEC Conf., The Hague, Netherlands, 1995, pp. 284–291.
[59] M.J. Hlavac, D. Feder, Proc. INTELEC Conf., Boston, MA, 1996, pp. 632–639.
[60] S.S. Misra, T.M. Noveske, A.J. Williamson, Proc. INTELEC Conf., Vancouver, Canada, 1994, pp. 250–255.
[61] J.M. Hawkins, L.O. Barling, Proc. INTELEC Conf., The Hague, Netherlands, 1995, pp. 271–276.